

Contact resistances in Trigate devices in a Non-Equilibrium Green's Functions framework

Léo Bourdet, Jing Li and Yann-Michel Niquet
University Grenoble Alpes, INAC/SP2M, L.Sim, Grenoble, France
CEA, INAC/SP2M, L.Sim, Grenoble, France
e-mail: yniket@cea.fr

As the gate length L of field-effect transistors is reaching the sub-20 nm range, the contact resistances are increasingly limiting the electrical performances of the devices. The “apparent” contact resistance R_c can be defined as the extrapolation to zero gate length of the total resistance of the device, $R(L) = V_{ds}/I_{ds}$, where I_{ds} is the drain current and V_{ds} the source-drain voltage. In the low field (low V_{ds}) regime, this contact resistance is dominated by *i*) the quality of the metal-semiconductor contact, *ii*) the transport through the lowly doped regions of the devices such as the spacers, and *iii*) the “ballistic” resistance of the channel. Although the latter is intrinsic to the channel, and has nothing to do with the design of the source/drain, it is usually mixed into the apparent contact resistance as it is independent on the gate length.

In this work, we compute components *ii*) and *iii*) of the contact resistance in Fully-Depleted Silicon-on-Insulator (FDSOI) Trigate devices in a Non-Equilibrium Green's Functions (NEGF) framework [1]. The channel is a rectangular nanowire with width W and height H , and the gate stack is made of 0.8 nm SiO_2 and 2.2 nm HfO_2 . It is connected to bulk source and drain contacts by 6 nm long spacers (see Fig. 1). Point-like dopants are added to the source and drain according to the different target distributions plotted in Fig. 2, in order to capture impurity scattering in these regions. Surface roughness, Remote Coulomb Scattering (RCS) in the channel, and electron-phonon interactions are also included in the simulations and have been calibrated on the experimental mobility. The current is computed with a NEGF code in the effective mass approximation.

At low bias, the resistance $R(L)$ of the devices is linear with L in the 20-100 nm range and can

therefore be extrapolated to $L = 0$ (Fig. 3). The contact resistance $R_c = R(L \rightarrow 0)$ in a 10x10 nm Trigate is plotted as a function of the carrier density in the channel in Fig. 4 (red line with dots), for the “Reference” doping profile of Fig. 2. It is compared to the ballistic resistance of the channel (no scattering), and to the contact resistance extracted in a device without surface roughness nor impurity scattering in the source/drain (continuous background dopant distributions). The contact resistance is much larger than the ballistic resistance, and is clearly limited by scattering by dopant impurities and surface roughness. It represents a significant part of the total resistance of a $L = 30$ nm long device (green line with diamonds). A careful analysis of the data (to be discussed at the conference) shows that the lowly doped spacers are the most resistive elements.

The contact resistances for the different doping profiles of Fig. 2 are plotted in Figs. 5, and for different nanowire cross sections in Fig. 6. R_c decreases when doping increases under the spacers, at the expense of a loss of electrostatic control (larger DIBL). Also, R_c increases when the cross sectional area decreases. Other results about the design of the spacers and the dependence of the contact resistance on V_{ds} will be discussed at the conference.

This work was supported by the French National Research Agency (ANR) project Noodles. The calculations were run on the TGCC/Curie machine thanks to allocations from PRACE and GENCI.

REFERENCES

- [1] Y.-M. Niquet, V.-H. Nguyen, F. Triozon, I. Duchemin, O. Nier, and D. Rideau, *Journal of Applied Physics* **115**, 054512 (2014).

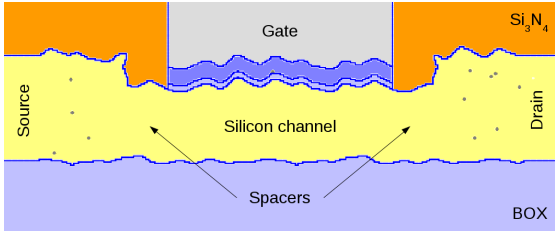


Fig. 1. A longitudinal cross section of a $W = 10 \times H = 10$ nm Trigate device, with overgrown source and drain contacts. The dots in the contacts are single dopant impurities. The spacers are 6 nm long.

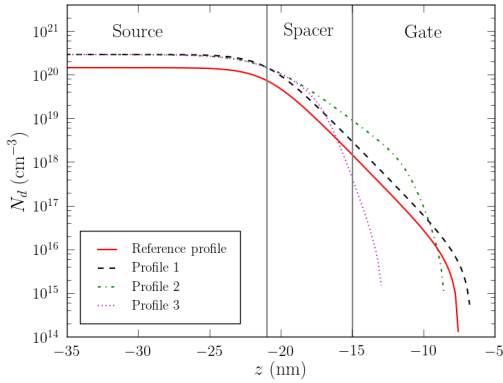


Fig. 2. Target doping profiles in the source of Fig. 1 (doping profiles are symmetric in the drain). They are used to generate random dopant distributions.

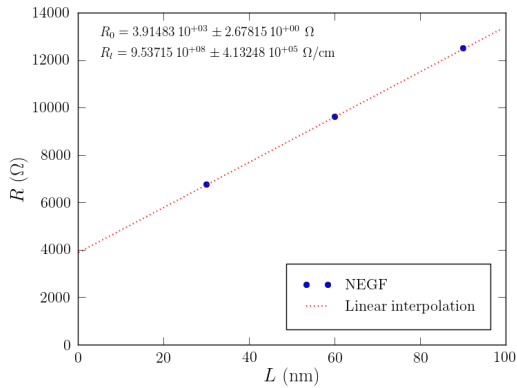


Fig. 3. The resistance $R(L)$ as a function of channel length L for a particular realization of the “Reference” doping profile of Fig. 2. The carrier density in the channel is $n = 10^{13} \text{ cm}^{-2}$. The contact resistance is the extrapolated $R_c = R(L \rightarrow 0)$, while the slope gives an estimate of the carrier mobility in the channel.

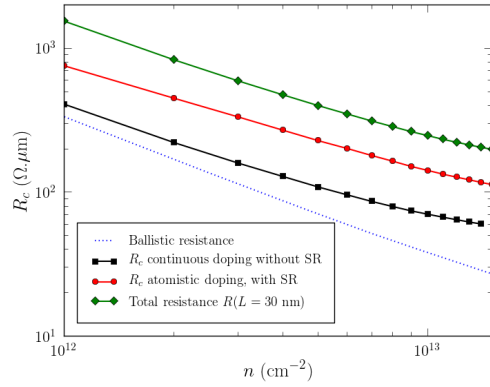


Fig. 4. The contact resistance R_c extracted from Fig. 3 as a function of the carrier density n in the channel. R_c is normalized to the effective width $W + 2H$ of the device. It is compared to the ballistic resistance of the channel, to the contact resistance extracted without surface roughness nor impurity scattering, and to the total resistance of a $L = 30$ nm long device.

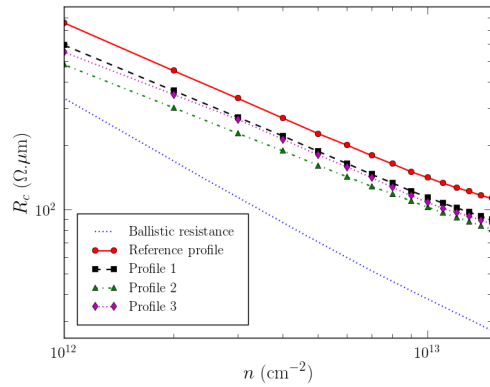


Fig. 5. The contact resistance R_c as a function of n for the different doping profiles of Fig. 2.

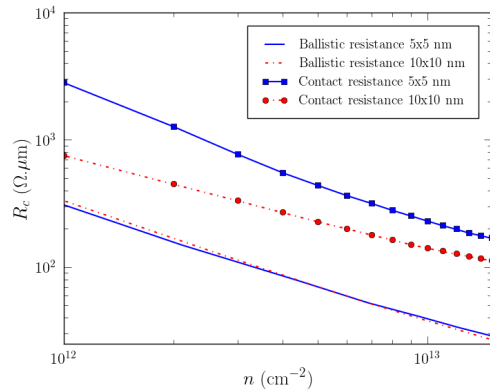


Fig. 6. The contact resistance R_c as a function of n for different nanowire cross sections. The target doping profile is the “Reference” profile of Fig. 2.